DOI: 10.1002/anie.200906200

Nanolithography

# Biomimetic Crystallization Nanolithography: Simultaneous Nanopatterning and Crystallization**

*Roberto de La Rica,* Kristina Ivana Fabijanic, Antonio Baldi, and Hiroshi Matsui**

Biomineralizing organisms such as starfish and marine sponges have evolved the capability to synthesize inorganic structures in mild conditions with an outstanding degree of complexity at the nano- and microscale.[1] Biomimetic routes in benign conditions (i.e. at room temperature and in aqueous solution), inspired by this natural crystal growth process, have been proposed to obtain technologically relevant materials, such as oxide semiconductors, with reduced cost and environmental impact.[2–7] Despite the great success of this bio-inspired approach, it would be desirable to find a methodology to pattern these biomimetically synthesized materials in desired shapes and dimensions for their integration in electronic components of complex circuits and microprocessors,[8] energy-storage systems,[9] solar cells,[10] optics,[11] and sensors.[12] For example, many biomineralization processes involve the formation of a highly hydrated amorphous phase, which can be further manipulated and crystallized in complex shapes in vitro by transport of the precursors controlled by the topology and chemical functions of biological substrates.[13–17] If the amorphous phase of an oxide semiconductor material (e.g. ZnO) could be isolated, nanopatterned, and crystallized at room temperature, the resulting semiconducting structures could be applied to upcoming nanoelectronics and nanooptics application with low cost and environmental impact.

To address this issue in bionanotechnology, we introduce a new lithography technique, biomimetic crystallization nanolithography (BCN), to fabricate oxide semiconductors and pattern them as nanowires on silicon at room temperature simultaneously. The characteristic features of BCN are the generation of relatively stable amorphous inks of ZnO, which are then nanopatterned with the tip of an atomic force microscope for a pen, similar to dip-pen nanolithography (DPN), and the simultaneous induction of crystallization with the AFM patterning process. In conventional DPN, materials such as molecules and polymers to be patterned are written as inks by using an AFM cantilever for a pen.[18] In BCN, materials in an amorphous state are used as inks to pattern them into desired shapes with the AFM tip. The novel feature of BCN is that the writing process induces the concomitant crystallization of the amorphous material to yield semiconducting nanopatterns (Figure 1). To draw crystalline ZnO nanowires on Si at room temperature by BCN, highly hydrated amorphous intermediates are required as inkwells for the writing on the substrate, and these amorphous inks are produced by the enzyme urease, which becomes the nucleation point for the reaction. After addition of the enzyme substrate urea, the urease on the Si substrate produces ammonia, and the resulting increase in pH value provides the necessary hydroxy groups for the growth of the oxide around the enzyme (Figure 1a).[7] Figure 2 shows that each enzyme creates an individual pH gradient, and these pH values near neutrality (yellow–light blue regions in Figure 2) generate low-reactivity intermediates[4,5] that lead to the formation of

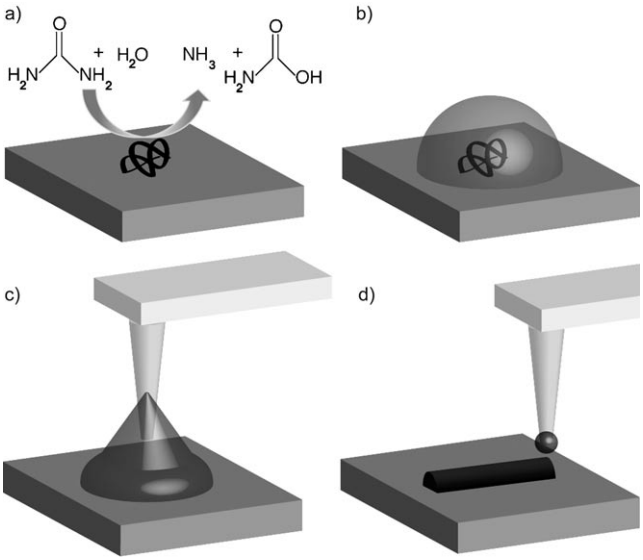


***Figure 1.*** Schematic of biomimetic crystallization nanolithography (BCN): a) The enzyme urease generates ammonia; b) the resulting pH gradient produces an amorphous ink of ZnO around the enzyme after adding Zn precursors; c) an AFM tip is inked with the amorphous particles; d) when a line is written with this ink in the contact mode of the AFM, the resulting nanowire is crystallized during the patterning.

[*] Dr. R. de La Rica, K. I. Fabijanic, Prof. H. Matsui
Department of Chemistry and Biochemistry
City University of New York–Hunter College
695 Park Avenue, New York, NY 10065 (USA)
Fax: (+1) 212-650-3918
E-mail: roberto.delarica@gmail.com
hmatsui@hunter.cuny.edu
Dr. A. Baldi
Department of Micro- and Nanosystems
Instituto de Microelectronica de Barcelona, IMB-CNM, CSIC
Campus UAB, 08193 Bellaterra (Spain)

[**] This work was supported by the US Department of Energy (DE-FG-02-01ER45935). Hunter College infrastructure is supported by the National Institutes of Health and the RCMI program (G12-RR-03037-24-2245476). R.R. acknowledges a postdoctoral fellowship from the Spanish Ministerio de Innovación y Ciencia and Fundación Española para la Ciencia y la Tecnología.

Supporting information for this article is available on the WWW under http://dx.doi.org/10.1002/anie.200906200.

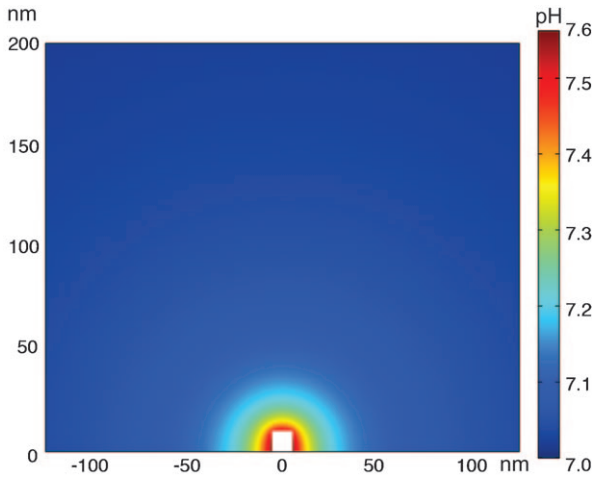


***Figure 2.*** Simulated pH gradient from the surface of the enzyme to the bulk of the solution. The numerical simulation of the diffusion pattern was carried out with a finite element method (COMSOL); urease is depicted as a cube of 11.5 nm side sitting on the substrate surface (details given in the Supporting Information).

the amorphous material on urease (Figure 1b, see also Sections 1 and 2 in the Supporting Information). Subsequently, the AFM tip is dipped into the amorphous ZnO ink (Figure 1c), and the oxide semiconductor nanopatterns are written in contact mode of AFM (Figure 1d).

Figure 3a shows an AFM image of an inkwell of amorphous ZnO, whose volume is large enough to draw micrometer-length nanowires of the semiconducting material

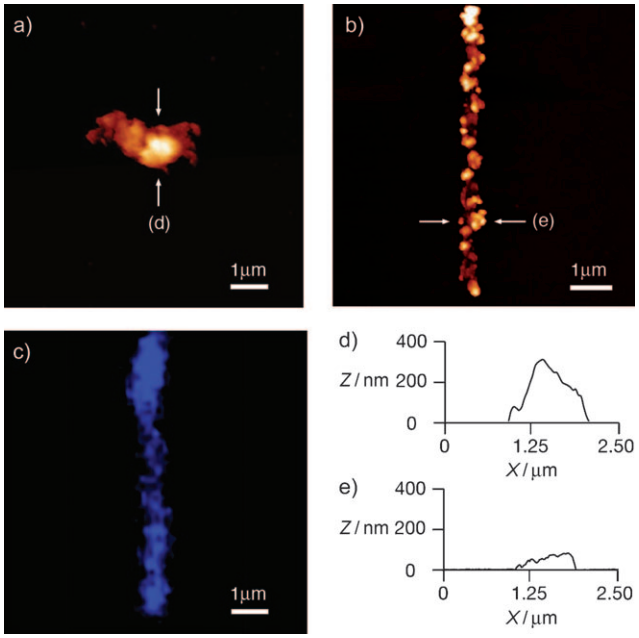


***Figure 3.*** ZnO nanopatterning by BCN with the tip velocity of 100 nm s$^{-1}$ and the tip force of approximately 100 nN: a) AFM image of the amorphous ZnO ink synthesized on the silicon substrate; b) AFM image after nanopatterning the amorphous ink as a line; c) fluorescence image showing the blue emission of the resulting ZnO nanowire; d) section analysis of amorphous ZnO/Zn(OH)$_x$ inks in (a); e) section analysis of crystalline ZnO line in (b).

(Figure 3d). No photoluminescence or contrast was detected when the substrate was imaged by either fluorescence microscopy or polarized light microscopy, thus indicating that the material was still in the amorphous phase (see also Section 2 in the Supporting Information). After the AFM tip was positioned at the center of the coated urease to load the amorphous ZnO, the ink was dragged by the AFM tip with a tip velocity of 100 nm s$^{-1}$ and a tip force of approximately 100 nN to yield ZnO lines as shown in Figure 3b. When the amorphous ink is patterned as a line by the AFM tip, the displacement of water molecules trapped in the amorphous material could accelerate the conversion to crystalline state.[13] Because the surface area of the nanopatterns in Figure 3b is higher than the surface area of the amorphous ink in Figure 3a and the friction between the tip and the surface generates heat, amorphous ZnO/Zn(OH)$_x$ displaces the excess solvent efficiently and the intermediate hydroxides could use this energy to eliminate water molecules and yield crystalline ZnO nanopatterns. To identify whether the patterning turns amorphous inks into crystalline ZnO lines, the emission of these lines was imaged by fluorescence microscopy. As shown in Figure 3c, the nanowire in Figure 3b emitted the characteristic blue emission of semiconducting zinc oxide at 457 nm,[19] thus demonstrating the concomitant crystallization of the material during the patterning process.

While the series of experiments in Figure 3 validated BCN for the simultaneous patterning and crystallization of submicrometer ZnO motifs, it would be desirable to downscale this patterning to the sub-100 nm range for state-of-the-art applications. Moreover, Figure 3b shows heterogeneous crystalline domains on the ZnO line as a result of the anisotropic nucleation of the crystals, which is consistent with recent reports that anisotropic morphologies are frequently observed in biomimetic syntheses of oxide semiconductors.[4,5] To decrease the dimensions of the nanowires and fabricate more homogeneous structures along the line during the writing process, the velocity of the patterning step was increased to 500 nm s$^{-1}$. As demonstrated in DPN, the tip velocity of the writing mode dictates the height and the uniformity of lines.[20] In our biomimetic DPN-like process, the fast tip velocity deposits less ink per unit area when the diffusion of ink from the tip to the receiving surface occurs at a constant speed, and the reduced amount of ink is expected to dehydrate rapidly to yield homogeneous morphologies via isotropic crystal growth. The ZnO line with monodisperse domain size in Figure 4a is consistent with this hypothesis. Although the dimensions of lines and nanoparticles on the line cannot be assessed because of the usual tip convolution problem, the diameter of the nanoparticles can be estimated from the height profiles to be 12 nm, and thus the line width was also estimated to be in the same order.[21] To demonstrate the capability of generating more-complex nanostructures in controlled dimensions by carefully tuning the parameters of the lithography step, an array of ZnO lines was generated by BCN at 500 nm s$^{-1}$ (Figure 4b). The average diameter of ZnO nanoparticles from 50 different areas was determined to be (12 ± 4) nm, therefore demonstrating the adequateness of BCN for the highly reproducible fabrication of nanostructures in the sub-100 nm range. The simultaneous synthesis and

  

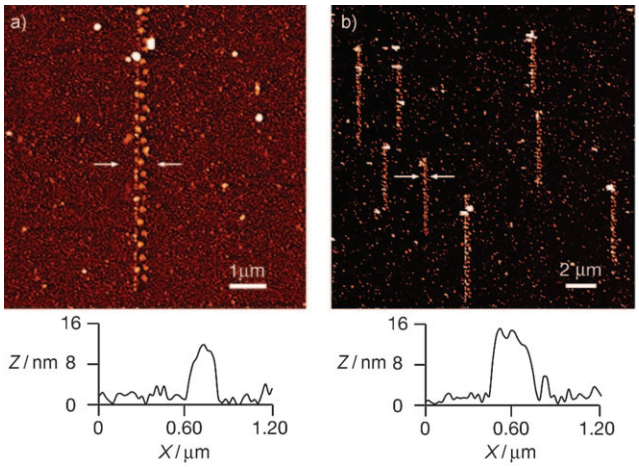


***Figure 4.*** ZnO nanopatterning by BCN with the tip velocity of 500 nm s$^{-1}$ and the tip force of approximately 100 nN: a) AFM image and height profile of a single line; b) AFM image and height profile of eight lines.

nanopatterning of nanocrystals with homogeneous morphology was possible because the deposition of a limiting amount of ink at high tip velocity resulted in isotropic crystal growth through fast nucleation,[22] and therefore this result shows that BCN can generate nanoscale patterns of crystalline oxide semiconductor materials by controlling the kinetics of crystal growth with the tip velocity in the writing process.

In summary, biomimetic crystallization nanolithography (BCN), a new nanofabrication methodology, was introduced to generate crystalline oxide semiconductor nanopatterns under mild conditions. In this approach, the material in the amorphous phase is first generated on substrates as an ink, and then patterned and crystallized in situ by writing the ink with an AFM tip. By carefully selecting the parameters of the lithography step such as tip velocity, the kinetics of crystal growth can also be controlled to yield oxide semiconductor nanocrystals in reproducible morphology and dimensions. The density of nanocrystals in a pattern could be tuned to be continuous by reducing the viscosity of the ink by varying the water content and polymerization degree of the amorphous intermediate. The inkwells can be generated at designated locations on the substrate by patterning urease with established electrostatic protein placement[23,24] and DPN techniques,[25] before triggering the mineralization process so that one can have more freedom to design further complex nanowire patterns by BCN.

## *Experimental Section*

To synthesize the amorphous ZnO ink, urease from jack beans was physisorbed on 1 cm$^2$ diced silicon wafers with a 350 nm layer of thermally grown silicon oxide by incubating them with a solution of the enzyme (0.1 μg mL$^{-1}$) in phosphate-buffered saline (0.01 M phosphate buffer, 0.0027 M KCl, 0.137 M NaCl; pH 7.4 tablets, Sigma) for 1 h. The urease-modified substrates were washed with deionized water, immersed in 100 mL of $NaNO_3$ (0.1 M), and then urea (10 mM) was added to create a suitable pH gradient for the preparation of amorphous ink. Urease was allowed to produce $NH_3$ around the enzyme for 30 s, and then $Zn(NO_3)_2{\cdot}(H_2O)_6$ (0.1 mM) was added with mixing for 1 h to synthesize amorphous ZnO inks on the surface of the silicon substrate. Subsequently, the substrates were washed with water and dried with streaming nitrogen for the following BCN step.

Biomimetic crystallization nanolithography and AFM analysis: After the amorphous inks were prepared on Si substrates, they were patterned by a stand-alone MFP-3D atomic force microscope (Asylum Research, Santa Barbara, CA). The position and length of these lines was defined by the MicroAngeloTM software. BCN was performed in contact mode by applying a tip force of approximately 100 nN and maximum tip velocities of 100 nm s$^{-1}$ or 500 nm s$^{-1}$. Ultrasharp silicon tips (MikroMasch) with a typical probe tip radius of 10 nm and a resonant frequency around 325 kHz were used for nanopatterning and imaging. For each tip, the spring constant was determined by the thermal noise method.[26] All topological images were taken in the tapping mode of AFM and treated with the WSxM software to enhance the contrast. The average height values were obtained by averaging the section analyses of more than eight lines. The variability in the measured dimensions was expressed as the standard deviation.

Received: November 4, 2009
Published online: January 19, 2010

**Keywords:** biomineralization · crystal growth · nanotechnology · scanning probe microscopy · zinc

[1] a) J. Aizenberg, J. C. Weaver, M. S. Thanawala, V. C. Sundar, D. E. Morse, P. Fratzl, *Science* **2005**, *309*, 275–278; b) J. C. Weaver, J. Aizenberg, G. E. Fantner, D. Kisailus, A. Woesz, P. Allen, K. Fields, M. J. Porter, F. W. Zok, P. K. Hansma, P. Fratzl, D. E. Morse, *J. Struct. Biol.* **2007**, *158*, 93–106.
[2] D. Kisailus, Q. Truong, Y. Amemiya, J. C. Weaver, D. E. Morse, *Proc. Natl. Acad. Sci. USA* **2006**, *103*, 5652–5657.
[3] D. Kisailus, J. H. Choi, J. C. Weaver, W. J. Yang, D. E. Morse, *Adv. Mater.* **2005**, *17*, 314–318.
[4] D. Kisailus, B. Schwenzer, J. Gomm, J. C. Weaver, D. E. Morse, *J. Am. Chem. Soc.* **2006**, *128*, 10276–10280.
[5] B. Schwenzer, J. R. Gomm, D. E. Morse, *Langmuir* **2006**, *22*, 9829–9831.
[6] H. Y. Bai, F. Xu, L. Anjia, H. Matsui, *Soft Matter* **2009**, *5*, 966–969.
[7] R. de La Rica, H. Matsui, *Angew. Chem.* **2008**, *120*, 5495–5497; *Angew. Chem. Int. Ed.* **2008**, *47*, 5415–5417.
[8] S. Y. Ju, A. Facchetti, Y. Xuan, J. Liu, F. Ishikawa, P. D. Ye, C. W. Zhou, T. J. Marks, D. B. Janes, *Nat. Nanotechnol.* **2007**, *2*, 378–384.
[9] Y. Qin, X. D. Wang, Z. L. Wang, *Nature* **2008**, *451*, 809–813.
[10] M. Law, L. E. Greene, J. C. Johnson, R. Saykally, P. D. Yang, *Nat. Mater.* **2005**, *4*, 455–459.
[11] M. H. Huang, S. Mao, H. Feick, H. Q. Yan, Y. Y. Wu, H. Kind, E. Weber, R. Russo, P. D. Yang, *Science* **2001**, *292*, 1897–1899.
[12] X. D. Wang, J. Zhou, J. H. Song, J. Liu, N. S. Xu, Z. L. Wang, *Nano Lett.* **2006**, *6*, 2768–2772.
[13] J. Aizenberg, D. A. Muller, J. L. Grazul, D. R. Hamann, *Science* **2003**, *299*, 1205–1208.
[14] J. Aizenberg, G. Lambert, S. Weiner, L. Addadi, *J. Am. Chem. Soc.* **2002**, *124*, 32–39.
[15] T. Tsuji, K. Onuma, A. Yamamoto, M. Iijima, K. Shiba, *Proc. Natl. Acad. Sci. USA* **2008**, *105*, 16866–16870.
[16] B. D. Reiss, C. B. Mao, D. J. Solis, K. S. Ryan, T. Thomson, A. M. Belcher, *Nano Lett.* **2004**, *4*, 1127–1132.
[17] F. C. Meldrum, H. Colfen, *Chem. Rev.* **2008**, *108*, 4332–4432.
[18] a) R. D. Piner, J. Zhu, F. Xu, S. H. Hong, C. A. Mirkin, *Science* **1999**, *283*, 661–663; b) S. W. Chung, D. S. Ginger, M. W.

  

Morales, Z. F. Zhang, V. Chandrasekhar, M. A. Ratner, C. A. Mirkin, *Small* **2005**, *1*, 64 – 69.
[19] M. L. Kahn, T. Cardinal, B. Bousquet, M. Monge, V. Jubera, B. Chaudret, *ChemPhysChem* **2006**, *7*, 2392 – 2397.
[20] L. R. Giam, Y. H. Wang, C. A. Mirkin, *J. Phys. Chem. A* **2009**, *113*, 3779 – 3782.
[21] C. Hahlweg, M. Gruhlke, H. Rothe, *Meas. Sci. Technol.* **2009**, *20*, 084018.
[22] J. Aizenberg, A. J. Black, G. M. Whitesides, *Nature* **1999**, *398*, 495 – 498.
[23] S. Kumagai, S. Yoshii, K. Yamada, N. Matsuoka, I. Fujiwara, K. Iwahori, I. Yamashita, *Appl. Phys. Lett.* **2006**, *88*, 153103.
[24] S. Yoshii, S. Kumagai, K. Nishio, A. Kadotani, I. Yamashita, *Appl. Phys. Lett.* **2009**, *95*, 133702.
[25] K.-B. Lee, J.-H. Lim, C. A. Mirkin, *J. Am. Chem. Soc.* **2003**, *125*, 5588 – 5589.
[26] E. D. Langlois, G. A. Shaw, J. A. Kramar, J. R. Pratt, D. C. Hurley, *Rev. Sci. Instrum.* **2007**, *78*, 093705.

  